

VOLUMETRIC LAGRANGIAN TEMPERATURE AND VELOCITY MEASUREMENTS IN THERMAL CONVECTION WITH TLCS

Theo Käufer, Christian Cierpka

Institute of Thermodynamics and Fluid Mechanics
Technische Universität Ilmenau
98693 Ilmenau, Germany
theo.kaeufer@tu-ilmenau.de

ABSTRACT

A Lagrangian method for simultaneously measuring temperature and velocity in a volume is presented, employing encapsulated Thermochromic Liquid Crystals (TLCs) as tracer particles for both variables. The experiments are performed in an equilateral hexagonal-shaped convection cell with a height of 60 mm and a distance of 104 mm between its parallel side walls, resulting in an aspect ratio of 1.73. A water-glycerol mixture is used as the fluid to match the density of the TLC particles. A densely connected neural network, trained on calibration data, is proposed to predict the temperature of individual particles based on their image and position in the color camera images, achieving uncertainties below 0.2 K over a temperature range of 3 K. The Shake-the-Box technique is used to determine the 3D position and velocity of the particles, which is then coupled with the temperature measurement approach. Applied to thermal convection at a Rayleigh number $Ra = 3.4 \times 10^7$ and a Prandtl number $Pr = 10.6$, the method allows for the visualization of detaching plumes and direct measurements of the convective heat transfer. Moreover, it is demonstrated that the approach enables the computation of statistics on convective heat transfer.

Introduction

Heat transfer is a crucial factor in various natural phenomena and engineering scenarios, and temperature variations often being the driving force behind fluid flow (Chillà & Schumacher, 2012). To understand these flows, it is essential to analyze both velocity and temperature data. A method for obtaining this information simultaneously is the combination of Particle Image Velocimetry (PIV) or Particle Tracking Velocimetry (PTV)/Lagrangian Particle Tracking (LPT) with Particle Image Thermometry (PIT), utilizing Thermochromic Liquid Crystals (TLCs) as the tracer particles (Dabiri, 2009). Due to their unique molecular arrangement, TLCs reflect light of different color depending on their temperature when exposed to white light (Tamaoki, 2001). Therefore, capturing temperature variations requires a color camera. The color reflection of the TLCs is influenced by further factors, including the angle of observation and the spectrum of illumination, making temperature calibration for the specific experimental setups essential (Moller *et al.*, 2019). This hybrid PIV/PIT technique has facilitated the examination of large-scale patterns in natural convection (Moller *et al.*, 2022; Käufer *et al.*, 2023) and turbulent heat flux in mixed convection (Mommert *et al.*, 2023). Moreover, recent advancements have expanded this method to

assess all three velocity components and the temperature at the particle level in thermal convection studies by integrating LPT with encapsulated TLCs, as described in a recent paper by Käufer & Cierpka (2024) and outlined in Fig. 1.

Experimental setup

The experiments were conducted in a Rayleigh-Bénard convection cell of hexagonal geometry, with dimensions of $h = 60$ mm in height and $w = 104$ mm in width. A schematic diagram offering a top view and detailing the coordinate system orientation is presented in Fig. 2. The experiment was carried out at a Rayleigh number $Ra = 3.4 \times 10^7$, defined by as $Ra = g\alpha\Delta T h^3 / \nu\kappa$, where g represents the acceleration due to gravity, α the thermal expansion coefficient, $\Delta T = T_h - T_c$ the temperature difference between the heating and cooling plates, h the height of the convection cell, ν the kinematic viscosity, and κ the thermal diffusivity, respectively. The experiment utilized a water-glycerol mixture with an 87:13 volume ratio as the working fluid, resulting in a Prandtl number $Pr = \nu/\kappa = 10.6$. This mixture was chosen to closely match the density of the encapsulated thermochromic liquid crystals used as tracer particles, which ranged in size from approximately 60 to 100 μm and were eliminated by a custom-made white light LED which was used in pulsed mode with a pulse width of 20 ms. The larger particle size was selected to ensure sufficient light reflection and to generate particle images of a size that allows for the reliable extraction of color information. This aspect is crucial for accurately determining the color and, thus, the temperature of individual particles. The flow within the cell was recorded using three cameras (PCO edge 5.5), one of which is color-sensitive due to a Bayer pattern in front of the sensors. All cameras were used with $f = 100$ mm focal length optics (Zeiss Milvus) and observed the region of interest under varying viewing angles but perpendicularly through the side-walls. By aligning the viewing direction perpendicularly to the sidewall and using large focal length optics, chromatic aberrations are minimized.

Temperature calibration and processing

To estimate the temperature from the particle images, a calibration that relates temperature and particle images is necessary. A flow chart of the procedure is shown within Fig. 3. For the calibration measurements, a uniform temperature was created in the convection cell by connecting both plates to a thermostat and using a magnetic stirrer to achieve a uniform

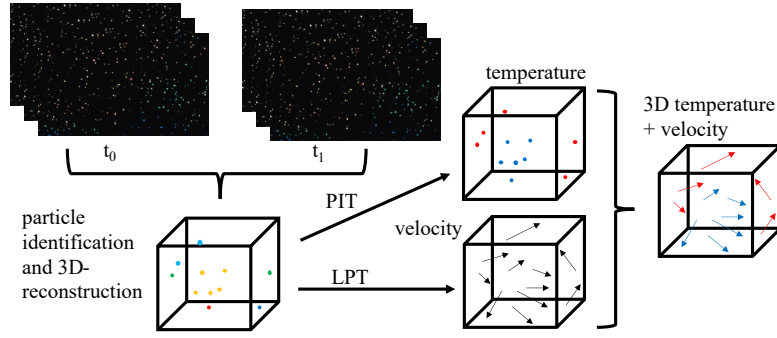


Figure 1. Schematic illustration of simultaneous temperature and velocity measurements. Particle images are captured using two monochrome cameras alongside a color camera. Particle identification and tracking are carried out by the proprietary Shake-the-Box software. Particle temperatures are derived from color particle images by employing a densely-connected artificial neural network. This figure is adapted from Käufer & Cierpka (2024).

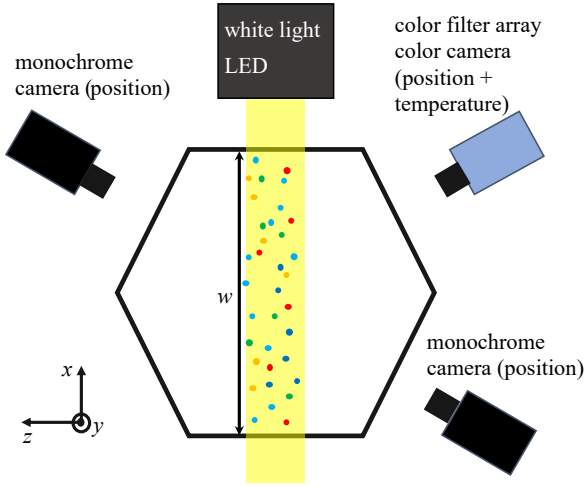


Figure 2. Schematic top-view illustration of the camera and light source arrangement with respect to the measurement domain. The illuminated domain where the measurements were performed is indicated, and the coordinate system is defined. The Figure is adapted from Käufer & Cierpka (2024).

temperature distribution. After stabilizing the temperature, color images of TLC particles were taken, and simultaneously, the plate temperature was measured with PT-100 thermistors to get a reference temperature T_{ref} . This procedure was repeated across temperatures from 19.7°C to 22.7°C in 0.2 K increments. Thereby, typical particle images at known temperatures are acquired. Exemplary particle images are shown in Fig. 4. After recording, color images were obtained from bilinear demosaicing of the color filter array (CFA) images. To identify individual particles, the color images were converted to grayscale and thresholded, and then a local maximum search was applied for peak detection. At the peak location 5×5 pixel particle images were extracted from the corresponding color image and normalized to compensate for variations of size and illumination. The normalized particle image, together with the position of the peak in the color camera image X and Y , was used to train a multi-layer perception after applying a train-test split of 90:10. The MLP was trained to predict the temperature using the reference temperature T_{ref} measured during the calibration as a target. For the machine learning procedure, the sci-kit learn package was used (Pedregosa *et al.*, 2011). After the training phase, the model's accuracy was tested, and the uncertainty was estimated by comparing the measured particle

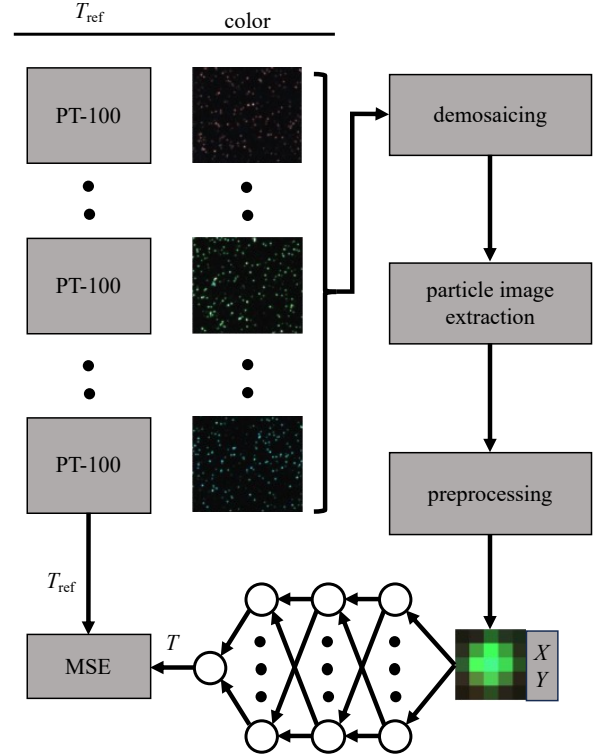


Figure 3. Flow chart of the temperature calibration procedure. To relate particle images and temperature, a densely connected neural network is trained on the particle images and their position in the color camera image at a known temperature. The target is the temperature measured by the temperature sensors in the plates during the calibration. MSE is the abbreviation for mean squared error. Figure taken from Käufer & Cierpka (2024).

temperatures T to the reference temperatures T_{ref} . The results are displayed in Fig. 5. It shows that the standard deviation of the measured particle temperature $\sigma(T)$ remains below 0.2 K across the temperature range, indicating a relative measurement uncertainty of about 6.5%. Furthermore, the mean absolute deviation $\langle |T_{\text{ref}} - T| \rangle$ is lower than the $\sigma(T)$ except for the highest calibration temperature, indicating little systematic deviation of T from T_{ref} . After the training, the neural network can be used to measure the temperature simultaneously and in combination with the velocity measurements obtained

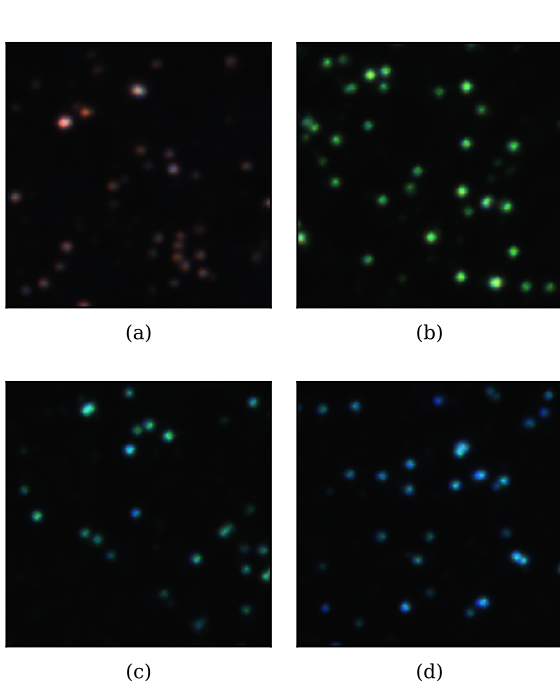


Figure 4. Exemplary images of TLC particles at 19.7 °C (a), 20.6 °C (b), 21.7 °C (c), and 22.7 °C (d). The color shift from red over green towards blue is recognizable with increasing temperature. This figure is adapted from Käufer & Cierpka (2024).

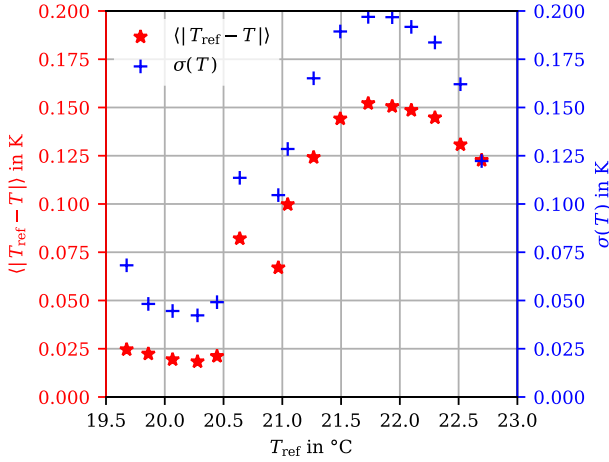


Figure 5. Plot of the mean absolute deviation between the reference and the measured particle temperature $\langle |T_{\text{ref}} - T| \rangle$ (red) and the standard deviation of the measured particle temperature σ_T (blue) for each reference temperature T_{ref} .

from the Shake-the-Box (STB) technique. Therefore, the 3D particle position is projected into the color camera image, and the particle image is extracted and processed in a similar way as the calibration data. After separately processing the particle velocities and temperatures, the temperature and velocity data were merged together. In a post-processing step, the temperature data are filtered by a sliding median filter along the trajectory, and short tracks are discarded, ensuring robust and accurate assessments of temperature and velocity. After post-processing, 998 snapshots with approximately 5000 particles each were available.

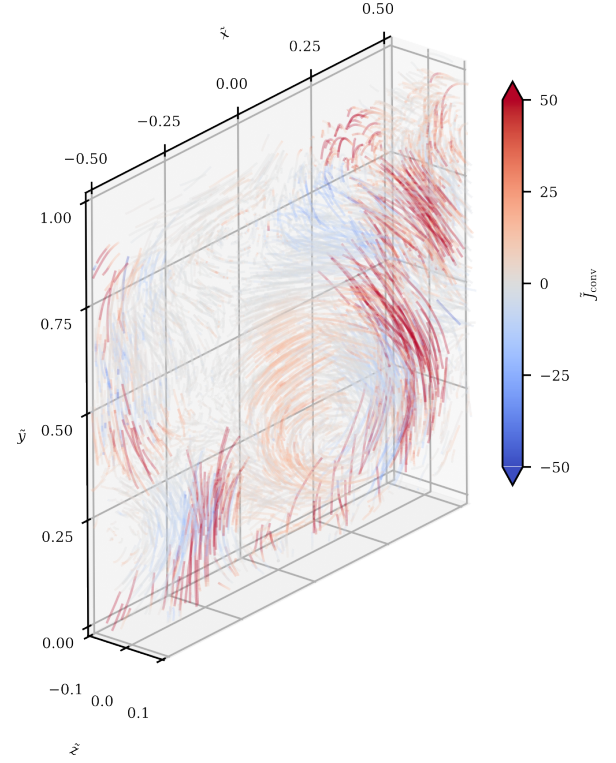


Figure 6. Trajectories of the convective heat transfer \tilde{J}_{conv} varying in length from 15 to 41 time steps. The thermal plumes stand out due to their enhanced heat transfer.

Results

To analyze the results the time t , the coordinate \mathbf{x} , velocity \mathbf{u} and temperature T are transferred into their non-dimensional representation according to

$$\tilde{t} = \frac{t}{\sqrt{h/\alpha g(T_h - T_c)}}, \quad (1)$$

$$\tilde{\mathbf{x}} = (\tilde{x}, \tilde{y}, \tilde{z}) = \frac{\mathbf{x}}{h}, \quad (2)$$

$$\tilde{T}(\tilde{\mathbf{x}}, \tilde{t}) = \frac{T(\tilde{\mathbf{x}}, \tilde{t}) - T_c}{\Delta T}, \quad (3)$$

$$\tilde{\mathbf{u}}(\tilde{\mathbf{x}}, \tilde{t}) = (\tilde{u}_x(\tilde{\mathbf{x}}, \tilde{t}), \tilde{u}_y(\tilde{\mathbf{x}}, \tilde{t}), \tilde{u}_z(\tilde{\mathbf{x}}, \tilde{t})) = \frac{\mathbf{u}(\tilde{\mathbf{x}}, \tilde{t})}{\sqrt{h\alpha g(T_h - T_c)}}. \quad (4)$$

After the non-dimensionalization, the dimensionless temperature fluctuation

$$\tilde{\Theta} = \tilde{T}(\tilde{\mathbf{x}}, \tilde{t}) - \langle \tilde{T}(\tilde{\mathbf{x}}, \tilde{t}) \rangle_{\tilde{\mathbf{x}}, \tilde{t}} \quad (5)$$

and the dimensionless convective heat transfer

$$\tilde{J}_{\text{conv}} = \sqrt{\text{RaPr}} \tilde{u}_y(\tilde{\mathbf{x}}, \tilde{t}) \tilde{\Theta}(\tilde{\mathbf{x}}, \tilde{t}) \quad (6)$$

can be calculated. To demonstrate that Fig. 6, presents the convective heat transfer \tilde{J}_{conv} along the particle trajectories. These paths vary in duration from 15 to 41 time steps. The figure highlights the separation of thermal plumes, distinguishable by their increased heat transfer compared to their surrounding. Furthermore, the joint measurement allows for the direct computation of statistics of the \tilde{J}_{conv} , similar to Shang *et al.*

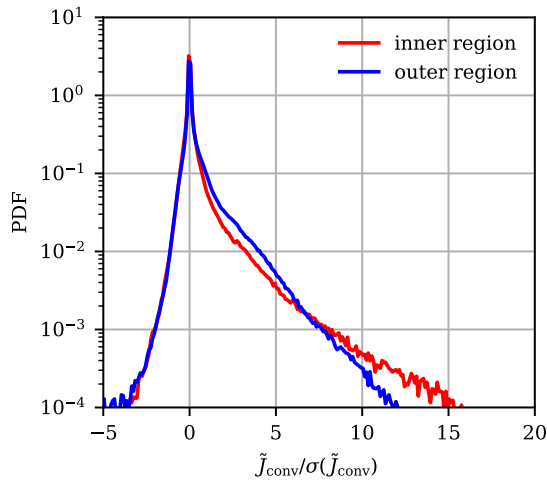


Figure 7. PDF of the normalized convective heat transfer \tilde{J}_{conv} for the inner $|\bar{x}| \leq 0.25$ (red) and outer $|\bar{x}| > 0.25$ (blue) region. The PDFs are skewed toward positive values since overall heat is transferred from the bottom toward the top.

(2004). To validate the results with literature, the probability density function (PDF) of the normalized convective heat transfer $\tilde{J}_{\text{conv}}/\sigma(\tilde{J}_{\text{conv}})$ for the inner $|\bar{x}| \leq 0.25$ (red) and outer $|\bar{x}| > 0.25$ (blue) region are shown in Fig 7. Both PDFs are skewed toward positive values, which aligns with the physics since overall heat is transferred from the bottom toward the top plate. Beyond that and albeit at different Ra and Pr, the shape of the PDFs agree qualitatively with the PDFs reported in Shang *et al.* (2004). This once more demonstrates the capabilities of the described method. $|\bar{x}| \leq 0.25$ (red) and outer region $|\bar{x}| > 0.25$ (blue)

Conclusion and Outlook

A novel method for simultaneously measuring temperature and velocity in 3D was presented. The technique is capable of direct measurements of the heat transfer along the particle trajectories in a volume, which is crucial for numerous technical applications. This opens avenues for a deeper understanding of convective heat transfer.

In the future, further improvements to the measurement technique are intended to be made by applying more color cameras and refining processing and post-processing. Additionally, the application of data assimilation techniques to interpolate the data onto an Eulerian grid for further analysis of the data is desired. For this purpose, physics-informed neural networks (Karniadakis *et al.*, 2021) or RBF with constraints (Sperotto *et al.*, 2024) are considered valuable tools. These methods are capable of leveraging the full potential of the 3D measurements and overcoming the limitation of planar data (Teutsch *et al.*, 2023).

REFERENCES

- Chillà, F. & Schumacher, J. 2012 New perspectives in turbulent Rayleigh–Bénard convection. *The European Physical Journal E* **35** (7), 58.
- Dabiri, D. 2009 Digital particle image thermometry/velocimetry: a review. *Experiments in Fluids* **46** (2), 191–241.
- Karniadakis, G. E., Kevrekidis, I. G., Lu, L., Perdikaris, P., Wang, S. & Yang, L. 2021 Physics-informed machine learning. *Nature Reviews Physics* **3** (6), 422–440.
- Käufner, T. & Cierpka, C. 2024 Volumetric Lagrangian temperature and velocity measurements with thermochromic liquid crystals. *Measurement Science and Technology* **35** (3), 035301.
- Käufner, T., Vieweg, P. P., Schumacher, J. & Cierpka, C. 2023 Thermal boundary condition studies in large aspect ratio Rayleigh–Bénard convection. *European Journal of Mechanics - B/Fluids* **101**, 283–293.
- Moller, S., Käufner, T., Pandey, A., Schumacher, J. & Cierpka, C. 2022 Combined particle image velocimetry and thermometry of turbulent superstructures in thermal convection. *Journal of Fluid Mechanics* **945**, A22.
- Moller, S., König, J., Resagk, C. & Cierpka, C. 2019 Influence of the illumination spectrum and observation angle on temperature measurements using thermochromic liquid crystals. *Measurement Science and Technology* **30** (8), 084006.
- Mommert, M., Niehaus, K., Schiepel, D., Schmeling, D. & Wagner, C. 2023 Measurement of the turbulent heat fluxes in mixed convection using combined stereoscopic PIV and PIT. *Experiments in Fluids* **64** (6), 111.
- Pedregosa, F., Varoquaux, G., Gramfort, A., Michel, V., Thirion, B., Grisel, O., Blondel, M., Prettenhofer, P., Weiss, R., Dubourg, V., Vanderplas, J., Passos, A., Cournapeau, D., Brucher, M., Perrot, M. & Duchesnay, É. 2011 Scikit-learn: Machine Learning in Python. *Journal of Machine Learning Research* **12** (85), 2825–2830.
- Shang, X.-D., Qiu, X.-L., Tong, P. & Xia, K.-Q. 2004 Measurements of the local convective heat flux in turbulent Rayleigh–Bénard convection. *Physical Review E* **70** (2), 026308.
- Sperotto, P., Ratz, M. & Mendez, M. A. 2024 SPICY: a Python toolbox for meshless assimilation from image velocimetry using radial basis functions. *Journal of Open Source Software* **9** (93), 5749.
- Tamaoki, N. 2001 Cholesteric Liquid Crystals for Color Information Technology. *Advanced Materials* **13** (15), 1135–1147.
- Teutsch, P., Käufner, T., Mäder, P. & Cierpka, C. 2023 Data-driven estimation of scalar quantities from planar velocity measurements by deep learning applied to temperature in thermal convection. *Experiments in Fluids* **64** (12), 191.